

Deviations from Fick's Law in Lorentz Gases

C. P. Lowe,¹ D. Frenkel,¹ and M. A. van der Hoef²

Received February 19, 1996; final August 20, 1996

We have calculated the self-dynamic structure factor $F(\mathbf{k}, t)$ for tagged particle motion in "hopping" Lorentz gases. We find evidence that, even at long times, the probability distribution function for the displacement of the particles is highly non-Gaussian. At very small values of the wave vector this manifests itself as the divergence of the Burnett coefficient (the fourth moment of the distribution never approaching a value characteristic of a Gaussian). At somewhat larger wave vectors we find that $F(\mathbf{k}, t)$ decays algebraically, rather than exponentially as one would expect for a Gaussian. The precise form of this power-law decay depends on the nature of the scatterers making up the Lorentz gas. We find different power-law exponents for scatterers which exclude certain sites and scatterers which do not.

KEY WORDS: Lorentz models; random media; Burnett coefficients; self-dynamic structure factor; long-time tails; computer simulation.

1. INTRODUCTION

When Alder and Wainwright⁽¹⁾ discovered the long-time tail in the velocity autocorrelation function of a hard-sphere fluid, they could hardly have expected that the stream of publications on the subject they started would decay so slowly. Much of our own work in this field has been motivated by the work on mode-coupling theory started by Matthieu Ernst and collaborators⁽²⁾ in 1970. In the present article we would have *liked* to present a study of a correlation function that does not have a long-time tail. However, we feel that this would be an unwarranted break with

¹ FOM Institute for Atomic and Molecular Physics, 1098 SJ Amsterdam, The Netherlands; e-mail: lowe@amolf.nl.

² University of Twente, Department of Chemical Technology, P.O. Box 217, 7500 AE Enschede, The Netherlands.

tradition,⁽³⁻¹¹⁾ so we will stick to long-time tails. First let us give a brief summary of the story so far.

The velocity autocorrelation function $C_v(t)$ is defined in terms of the instantaneous particle velocity $\mathbf{v}(t)$ as follows:

$$C_v(t) = \frac{1}{d} \langle \mathbf{v}(0) \cdot \mathbf{v}(t) \rangle \quad (1)$$

where d is the dimensionality of the system. It can in turn be related to a more macroscopically observable quantity, the mean square displacement $\Delta(t)$,

$$\frac{\Delta(t)}{2dt} = \int_0^t C_v(t') dt' - \frac{1}{t} \int_0^t t' C_v(t') dt' \quad (2)$$

At long times the second term (almost always) goes to zero, so, from the Einstein definition of the diffusion coefficient D , we have

$$D = \lim_{t \rightarrow \infty} \frac{\Delta(t)}{2dt} = \int_0^{\infty} C_v(t') dt' \quad (3)$$

the so-called Green-Kubo relation between the velocity autocorrelation function (VACF) and the diffusion coefficient.

If a process is Markovian (i.e., what happens at any given instant is uncorrelated with what happened at any previous instant), then these correlations should decay away exponentially. What Alder and Wainwright found was that the VACF in a hard-sphere fluid, rather than decaying exponentially as expected (particle motion in fluids was assumed to be Markovian at the time), decayed with a power-law form, $C_v(t) \sim t^{-d/2}$. They also provided a quantitative explanation for the effect in terms of the slow decay of the hydrodynamic fields set up by an object moving in a fluid. In light of this observation a rethinking of kinetic theory was necessary. More formal theoretical explanations, based on kinetic⁽¹²⁾ and mode-coupling⁽²⁾ theories, soon followed. Rather than being unique to the VACF, long-time tails were predicted for other time correlation functions (for instance, the stress-stress correlation function⁽²⁾ and the angular velocity autocorrelation function⁽¹³⁾). In the intervening years these predictions have been extensively tested, by computer simulation^(3-5, 9-11, 14) and, for the VACF of colloidal particles, by experiment.⁽¹⁵⁻¹⁹⁾ A computer simulation technique developed by Frenkel and Ernst (moment propagation⁽²⁰⁾) allowed the VACF for particles in lattice-based model fluids to be calculated to an extremely high degree of accuracy. In these fluids it proved

possible to test even the most subtle details of mode-coupling theory,⁽³⁻⁵⁾ including the renormalization of the VACF in two dimensions.^(4, 11)

Following the discovery of the long-time tail in simple fluids, Ernst and Weijland⁽²¹⁾ predicted the existence of a long-time tail in the even simpler system that we consider in this article—namely the Lorentz gas. This family of models, originally introduced by Lorentz to study diffusion in binary mixtures of gases, are all characterized by point particles moving in an array of fixed obstacles. Whereas in the simple fluids (discussed above) momentum is conserved, in Lorentz gases it is not. The origin of the long-time tail is therefore quite different and so is its sign. Ernst and Weijland⁽²¹⁾ predicted a negative tail of the form $C_v(t) \sim -t^{-(d+2)/2}$. Although initially simulations appeared to find deviations from this prediction,^(22, 23) the most recent simulations^(6, 7) seem to confirm the algebraic decay predicted by Ernst and Weijland. The best available theory for the constant of proportionality, or coefficient, of the decay⁽²⁴⁾ predicts values in full agreement with simulation⁽²⁵⁾ (although this requires the numerical evaluation of fluctuations in the diffusion coefficient, analytic results are still rather poor⁽⁷⁾).

The VACF tells us something, but not everything, about tagged particle motion. If one knows the VACF one can determine the mean square displacement using Eq. (2). Of course, this is only part of the story. The mean square displacement is one property of the distribution function $P(\mathbf{r}, t)$, defined as the probability that a particle initially located at the origin is at position \mathbf{r} at some later time t . The function $P(\mathbf{r}, t)$ tells us everything we could hope to know about tagged particle motion. If Fick's law is valid (i.e., the process is Markovian), then $P(\mathbf{r}, t)$ will be a solution of the diffusion equation,

$$\frac{dP(\mathbf{r}, t)}{dt} = D \nabla^2 P(\mathbf{r}, t) \quad (4)$$

with the diffusion coefficient given by Eq. (3). But, as Eq. (3) shows, the diffusion "constant" can only be considered constant on time scales long compared to the time it takes the VACF to decay. On these grounds alone, Fick's law, Eq. (4), can only be valid on certain time scales.

Rather than studying $P(\mathbf{r}, t)$ itself, we have studied its Fourier transform, $F(\mathbf{k}, t)$,

$$F(\mathbf{k}, t) = \int_{-\infty}^{\infty} P(\mathbf{r}, t) \exp(i\mathbf{k} \cdot \mathbf{r}) d\mathbf{r} \quad (5)$$

This quantity, known as the self-dynamic structure factor (SDSF), can be determined experimentally by, for instance, photocorrelation spectroscopy.

The SDSF provides a particularly convenient means of extracting the moments of $P(\mathbf{r}, t)$ because, by expanding the exponential in Eq. (5) in terms of \mathbf{k} , $F(\mathbf{k}, t)$ can itself be expressed in terms of the moments for $P(\mathbf{r}, t)$. This is most conveniently done by means of a cumulant expansion about a Gaussian, for which the first two terms are

$$F(k, t) = \exp \left(-\frac{k^2}{2!} \langle r_x(t)^2 \rangle + \frac{k^4}{4!} (\langle r_x(t)^4 \rangle - 3 \langle r_x(t)^2 \rangle^2) + O(k^6) \right) \quad (6)$$

and the α subscripts refer to one component.

If the distribution is Gaussian, then only the first term in the expansion is nonzero. The solution to the diffusion equation, Eq. (4), starting from a delta function initial distribution, is itself a Gaussian—so Fickian behavior corresponds to

$$F(k, t) = \exp(-k^2 Dt) \quad (7)$$

The higher order terms in Eq. (6) reflect deviations in $P(\mathbf{r}, t)$ from a Gaussian or, equivalently, deviations from Fick's law. A more general form of Eq. (7), which accounts for the deviations of the first and second terms in the cumulant expansion from Fickian values, is

$$F(k, t) = \exp \left(-k^2 \int_0^t D(t') dt' + k^4 \int_0^t B(t') dt' + O(k^6) \right) \quad (8)$$

from which it is convenient to define a "time- and wavevector-dependent" diffusion coefficient $D(k, t)$,

$$D(k, t) = -\frac{d}{dt} \left(\frac{\ln F(k, t)}{k^2} \right) = D(t) - B(t) k^2 + O(k^4) \quad (9)$$

If a process is Fickian, then $D(k, t)$ reduces to the diffusion coefficient. By definition the functions $D(t)$ and $B(t)$, the time-dependent diffusion and Burnett coefficients, respectively, are given by

$$D(t) = \frac{1}{2!} \frac{d}{dt} \langle r_x(t)^2 \rangle \quad (10)$$

$$B(t) = \frac{1}{4!} \frac{d}{dt} (\langle r_x(t)^4 \rangle - 3 \langle r_x(t)^2 \rangle^2) \quad (11)$$

At long times the time derivative of $D(t)$, which we denote $C_D(t)$, is directly proportional to the VACF [see Eq. (2)]. Similarly, the time

derivative of $B(t)$, which we denote by $C_B(t)$, is proportional to a (four-point) velocity correlation function. Interestingly, the theoretical prediction is that $B(t)$ diverges logarithmically in two dimensions, or, equivalently, that the correlation function $C_B(t)$ decays as $1/t$. This implies that in a two-dimensional Lorentz gas the fourth moment is never characteristic of a Gaussian. This prediction was tested in a computer simulation of a continuous Lorentz gas by Alley.⁽²⁶⁾ The results, while strongly suggesting that the Burnett coefficient was indeed diverging, did not confirm the form of the divergence. Similar observations of large non-Gaussian effects in Lorentz gases have recently been reported by Cohen and Wang.⁽²⁷⁾

Our aim in this article is to examine deviations from Fick's law in a variant of the Lorentz gas known as the "hopping" Lorentz gas. We will start by describing the two versions of this model that we have studied (the "excluded-site" and "broken-bond" models) and the method that we have used to calculate the SDSF. We then describe the results of our calculations (performed in both two and three dimensions) and discuss what they imply with respect to Fick's law.

2. DESCRIPTION OF THE MODEL

We have calculated the self-dynamic structure factor for two versions of the "hopping" Lorentz gas. In the hopping Lorentz gas a point particle (the "walker") performs a random walk on a lattice until it encounters a fixed scatterer. At this point it is reflected (see Fig. 1). The fixed scatterers themselves are randomly distributed on the lattice (in our case a face-centered hypercube projected onto either two or three dimensions). The two variants we consider differ only in the type of scatterer. The first type of scatterers consist of excluded lattice sites. Any random walker which tries to reach one of these excluded sites is reflected at half a time step and, over a full time step, returns to its original site. The second type of scatterers are just bonds which are "broken" at random. Any random walker which tries to travel along one of these broken bonds is reflected at half a time step, so, again, over a full time step, it returns to its original site. The fundamental difference between the two systems is that for the excluded site model there are excluded areas (or volumes) which no walker can ever visit, whereas for the bond model all sites are accessible (if the density is low enough to avoid trapping). Consequently the stationary distribution for the bond model is uniform, whereas for the site model it is not. This is known to influence the behavior of the VACF,⁽⁶⁾ although not the asymptotic exponent of the algebraic decay.

For a given configuration of scatterers, the best possible statistics we could obtain would come from averaging over all possible random walks

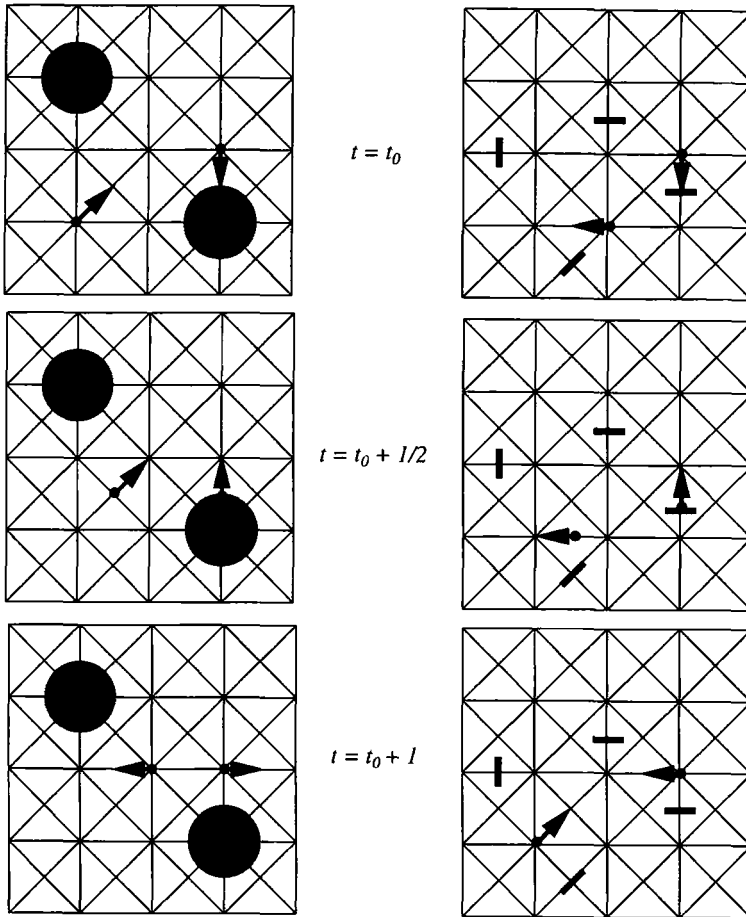


Fig. 1. Schematic representation of the hopping Lorentz gas with excluded-site scatterers (left) and broken-bond scatterers (right).

in the system. To do this explicitly would be prohibitively time-consuming, but fortunately, by taking a given wave vector, the moment propagation method⁽²⁰⁾ allows us to do this in one go. The technique has been employed to calculate the VACF in both Lorentz gases and lattice gases and can be applied in essentially the same manner to calculate the SDSF. The SDSF, defined in Eq. (5), is just a time correlation function with the same form as the VACF, but involving the particle positions \mathbf{r} , rather than velocities

$$F(\mathbf{k}, t) = \langle \exp(-i\mathbf{k} \cdot \mathbf{r}_i(0)) \exp(i\mathbf{k} \cdot \mathbf{r}_i(t)) \rangle \quad (12)$$

The trick for the VACF is to propagate in time a quantity $P_{\mathbf{r}}(\mathbf{r}, t)$, defined as the *weighted* sum of the probabilities of all trajectories ending at position \mathbf{r} at time t . Once specified, $P_{\mathbf{r}}(\mathbf{r}, t)$ can be propagated forward in time according to

$$P_{\mathbf{r}}(\mathbf{r}, t+1) = \sum_{\mathbf{j}_{\text{nb}}} p_{-\mathbf{j}_{\text{nb}}}(\mathbf{r}+\mathbf{j}, t) P_{\mathbf{r}}(\mathbf{r}+\mathbf{j}, t) + \sum_{\mathbf{j}_{\text{b}}} P_{\mathbf{j}_{\text{b}}}(\mathbf{r}, t) P_{\mathbf{r}}(\mathbf{r}, t) \quad (13)$$

where \mathbf{j}_{nb} is the set of unbroken links connecting each site to its neighbours, \mathbf{j}_{b} is the set of broken links, and $p_{\mathbf{j}}(\mathbf{r}, t)$ is the probability that a particle located at position \mathbf{r} at time t subsequently moves along link \mathbf{j} . The second term in Eq. (13) reflects the fact that a particle which sets off along a broken link returns to its original site. For an unbiased random walk, the probability $p_{\mathbf{j}}(\mathbf{r}, t)$ is particularly simple—it is just equal to $1/b$, where b is the number of directions along which the particle can travel. In the case of the VACF the weight applied to the trajectories is just equal to the initial velocity component of the particles, $u_x(0)$. It is specified by directly calculating $P_{\mathbf{r}}(\mathbf{r}, 1)$ —which can then be propagated forward in time using Eq. (13). Once we know $P_{\mathbf{r}}(\mathbf{r}, t)$, the contribution to the VACF from all trajectories ending at \mathbf{r} is just equal to the sum of the weighted probabilities correlated with the particle velocities $u_x(t)$ at position \mathbf{r} . All that remains is to sum over the N (free) sites in the system and average. Examining Eq. (12), it follows that, in order to calculate the SDSF at a fixed value of \mathbf{k} , we follow the same procedure as for the VACF, but weight the trajectories with $\exp(-i\mathbf{k} \cdot \mathbf{r}_i(0))$ and correlate with $\exp(i\mathbf{k} \cdot \mathbf{r}_i(t))$. The latter is of course the same for all trajectories ending at \mathbf{r} , so can be replaced by $\exp(i\mathbf{k} \cdot \mathbf{r})$. The equations we explicitly solve in order to calculate the SDSF in the hopping Lorentz gas are therefore

$$P_{\mathbf{r}}(\mathbf{r}, 1) = \frac{1}{b} \sum_{\mathbf{j}_{\text{nb}}} \exp(-i\mathbf{k} \cdot (\mathbf{r}+\mathbf{j})) + \frac{1}{b} \sum_{\mathbf{j}_{\text{b}}} \exp(-\mathbf{k} \cdot \mathbf{r}) \quad (14)$$

$$P_{\mathbf{r}}(\mathbf{r}, t+1) = \frac{1}{b} \sum_{\mathbf{j}_{\text{nb}}} P_{\mathbf{r}}(\mathbf{r}+\mathbf{j}, t) + \frac{1}{b} \sum_{\mathbf{j}_{\text{b}}} P_{\mathbf{r}}(\mathbf{r}, t) \quad (15)$$

$$F(\mathbf{k}, t) = \frac{1}{N} \sum_{\mathbf{r}} P_{\mathbf{r}}(\mathbf{r}, t) \exp(i\mathbf{k} \cdot \mathbf{r}) \quad (16)$$

For the broken-bond model the set of sites \mathbf{r} consists of all the nodes on the lattice, whereas for the excluded site model it consists of just the nonexcluded sites. There are two things to note about Eq. (15). First, it conserves the sum over the system of $P_{\mathbf{r}}(\mathbf{r}, t)$. Second, it has a uniform

equilibrium distribution (within the accessible space). At infinitely long times it will therefore decay to a constant value P_{tr}^∞ given by

$$P_{tr}^\infty = \frac{1}{N} \sum_{\mathbf{r}} P_{tr}(\mathbf{r}, 1) \quad (17)$$

This means that the SDSF decays to

$$\lim_{t \rightarrow \infty} F(\mathbf{k}, t) = \frac{P_{tr}^\infty}{N} \sum_{\mathbf{r}} \exp(i\mathbf{k} \cdot \mathbf{r}) \quad (18)$$

which, for any given realization of the excluded-site model, is only zero in the thermodynamic limit. This is physically sensible—the SDSF decays to the Fourier transform of the nonexcluded area of the system (multiplied by a constant), which, if the scatterers are randomly distributed, is only zero in this limit. In order to correct for this in the (finite-sized) simulation, the function we actually calculate is

$$F_{\text{calc}}(\mathbf{k}, t) = F(\mathbf{k}, t) - \lim_{t \rightarrow \infty} F(\mathbf{k}, t) \quad (19)$$

although for future purposes we drop the subscript. No similar correction is required for the broken-bond model.

3. RESULTS

First we consider the results of simulations performed on a two-dimensional lattice consisting of 502^2 lattice sites. Applying periodic boundary conditions, we used the scheme outlined above to calculate $F(\mathbf{k}, t)$. The position vectors \mathbf{r} were calculated from an origin located at one corner of the simulation square. All the periodic images of a random walker make the same contribution to $F(\mathbf{k}, t)$, so we can just consider the walkers within the simulation square. We only performed the calculation for times up to the minimum time required for a random walker to cross the simulation square (i.e., 502 time steps), so we can completely exclude the influence of the periodic boundary conditions from our results. The wave vector \mathbf{k} was chosen to lie along one of the Cartesian axes (so from now on we can treat it as a scalar, k) and we performed the calculation over a wide range of k values. The scatterer density was chosen to be high enough to be able to see any interesting effects, but still well below the critical density (at which the diffusion coefficient vanishes and trapped particles might make an anomalous contribution to the SDSF). Specifically,

for the excluded-site model we studied a system in which 10% of the total number of sites were excluded and for the broken-bond model a system in which 10% of the bonds were broken. All the results described in this article were obtained by averaging the SDSF over 10–20 configurations of scatterers.

For the excluded-site model we first tested the procedure outlined above for excluding finite-size effects. To do this we repeated the calculation on a smaller system (201^2) where the finite-size correction is larger. We found that, up to the minimum time required for a walker to cross the box, the corrected SDSF for the two systems (201^2 and 502^2) was identical. From this we concluded that our approach was satisfactory. The results we obtained for the time- and wavevector-dependent diffusion coefficient in the larger system are shown in Fig. 2. The values have also been normalized by the diffusion coefficient of the walkers in the absence of any obstacles, D_0 . Defining our units such that the time step and lattice spacing are both unity, the “bare” diffusion coefficient D_0 is equal to $1/4$ for all the work we report here. Remembering that Fick's law corresponds to $D(k, t)$ being a constant (a horizontal line in Fig. 2), the deviations, particularly at large values of k , are clearly pronounced. We start our analysis by looking at

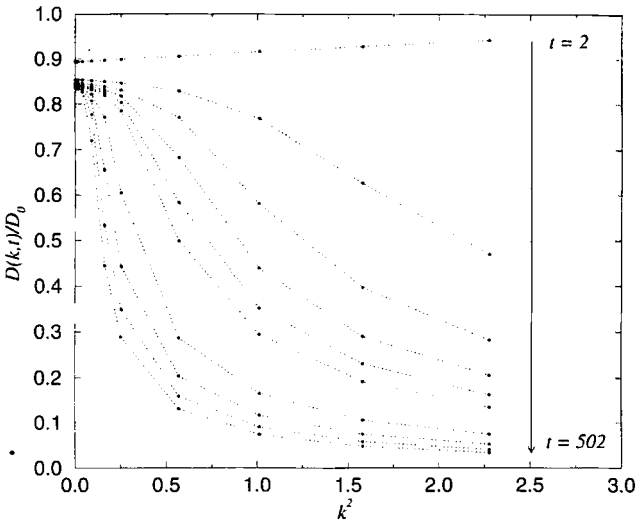


Fig. 2. The time- and space-dependent diffusion coefficient $D(k, t)$, normalized by the diffusion coefficient of the walker in the absence of the scatterers D_0 , and plotted as a function of the square of the wave vector k . The system consisted of a two-dimensional Lorentz gas, with excluded-site scatterers occupying 10% of the total lattice sites. The curves, from top to bottom, correspond to times of 2, 22, 42, 62, 82, 102, 202, 302, 402, and 502 time steps. The dotted lines are a guide to the eye and the errors are of the order of the line thickness.

small values of k (for which $k^2 < 1/Dt$), corresponding to (real-space) length scales greater than the mean-squared displacement. In Fig. 3 we have plotted the time- and wavevector-dependent diffusion coefficient at small values of k as a function of k^2 . On the basis of the cumulant expansion (8), the data should be linear with the intercept at $k=0$, giving $D(t)$ and minus the slope giving the Burnett coefficient. The straight lines in Fig. 3 are linear fits to the data and it is clear that the intercepts are moving to lower values of $D(t)$ at longer times. This is the effect of the (negative) long-time tail in the VACF. What is less obvious is that the (negative) slope of the lines is increasing. From the fits shown in Fig. 3 we have calculated the correlation functions $C_D(t)$ and $C_B(t)$, associated with the time-dependent diffusion and Burnett coefficients, respectively. These are plotted in log-log form in Fig. 4. Performing linear fits to the data, we obtained exponents of -1.95 ± 0.06 and -1.02 ± 0.04 , compared with the theoretically predicted values of -2 and -1 . The exponent of -1 in the decay of $C_B(t)$ confirms that the time-dependent Burnett coefficient is diverging as $\ln t$. Since $C_D(t)$ is proportional to the VACF, extracting it from the SDSF amounts to a rather inefficient calculation of the long-time

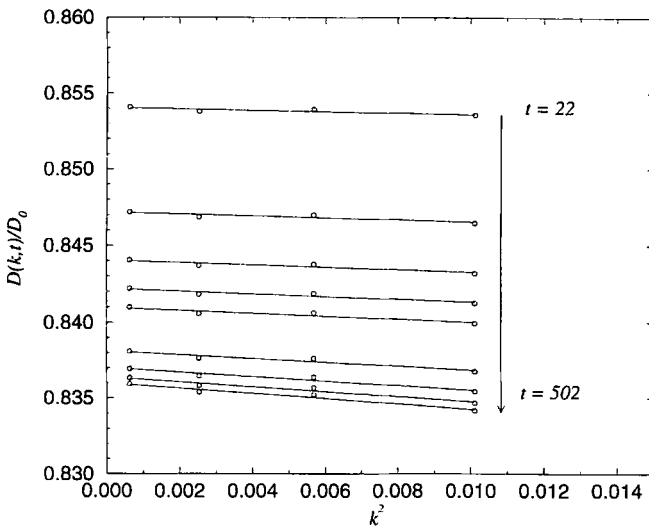


Fig. 3. The time- and space-dependent diffusion coefficient $D(k, t)$ normalized by the diffusion coefficient of the walker in the absence of the scatterers, D_0 , and plotted in as a function of the square of the wave vector k for small values of k . The system consisted of a two-dimensional Lorentz gas, with excluded-site scatterers occupying 10% of the lattice sites. The data, from top to bottom, correspond to times of 22, 42, 62, 82, 102, 202, 302, 402, and 502 time steps. The errors are of the order of the symbol size and the solid lines are linear least squares fits to the data.

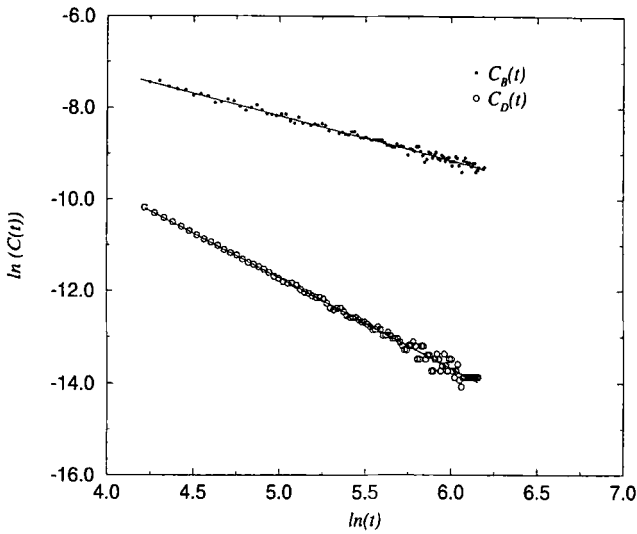


Fig. 4. Log-log plot of the correlations functions $C_D(t)$ and $C_\beta(t)$ associated with the time-dependent diffusion and Burnett coefficients, respectively. The solid lines are linear least squares fits to the data.

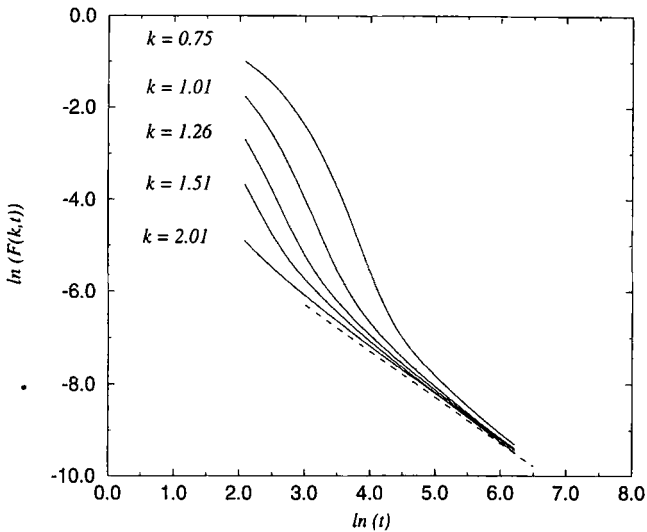


Fig. 5. Log-log plot of the self-dynamic structure factor $F(k,t)$ at various (large) k values, in the two-dimensional system with excluded-site scatterers. The dashed line is a line with a gradient of -1 , provided for comparison.

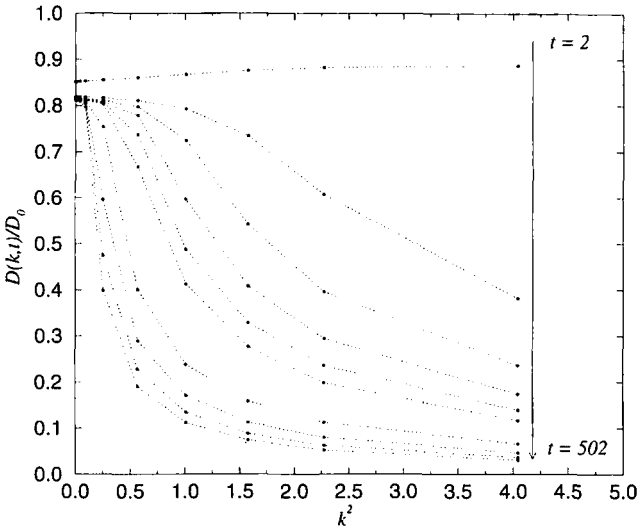


Fig. 6. The time- and space-dependent diffusion coefficient $D(k, t)$, normalized by the diffusion coefficient of the walker in the absence of the scatterers, D_0 , and plotted as a function of the square of the wave vector k . The system consisted of a two-dimensional Lorentz gas with broken-bond scatterers, the broken bonds making up 10% of the total for the lattice. The curves, from top to bottom, correspond to times of 2, 22, 42, 62, 82, 102, 202, 302, 402, and 502 time steps. The dotted lines are a guide to the eye and the errors are of the order of the line thickness.

tail in VACF. The fact that we do get the correct power law does, however, serve as a useful test.

If we now examine the origin of the pronounced deviations from Gaussian behavior at larger values of k ($k^2 \gg 1/Dt$), corresponding to real-space length scales smaller than the root mean squared displacement, then we find a surprising result. In Fig. 5 we have plotted the SDSF in log-log form. Clearly the SDSF itself is approaching an algebraic decay with an exponent of -1 . To our knowledge this has not been predicted theoretically. One further thing to notice is that the coefficient of the "tail" in the SDSF appears to be independent of k . This suggests that, in real space, this effect is localized near the origin. One would not expect the distribution to be Gaussian on very short length scales because of the excluded area of the scatterers themselves. For instance, any particle which starts on the surface of a scatterer must, even at infinitely long times, have a distribution containing a "hole" adjacent to the origin. The Fourier transform does not distinguish between a distribution with a hole to the left of the origin and a distribution with a hole to the right, so it is unlikely this effect will cancel due to ensemble averaging.

This brings us to the broken-bond model, which contains no excluded-area effects. The results we obtained for the time- and wavevector-dependent diffusion coefficient are shown in Fig. 6. Qualitatively, they look similar to the results for the excluded site model. We have a plateau, at sufficient small values of k , but pronounced non-Gaussian effects at large k . For this model we have not tried to extract the time dependence of the Burnett coefficient. The divergence, while still visible, is rather weak compared to the level of statistical error in the results at small k . However, for this model we are more interested in the larger k region ($k^2 > 1/Dt$). Specifically, does the tail effect we saw in the excluded-site model disappear? In Fig. 7 we have plotted $F(k, t)$ against t in log-log form for various (large) values of k and the answer appears to be: not quite. Once more we see an approach to a power-law decay, but with a different exponent. This time the exponent is -2 (for the excluded-site model it was -1). It is also clear from Fig. 7 that this time the tail coefficient is not independent of k . A careful analysis suggests that it is proportional to $1/k^2$.

To see if the above observations are unique to a two-dimensional system we repeated the calculation for two relatively large wave vectors in a three-dimensional system. Again we limited the time up to which we calculated $F(k, t)$ to the time taken for a walker to cross the simulation box. The density of objects was 10% of excluded sites or 10% of broken

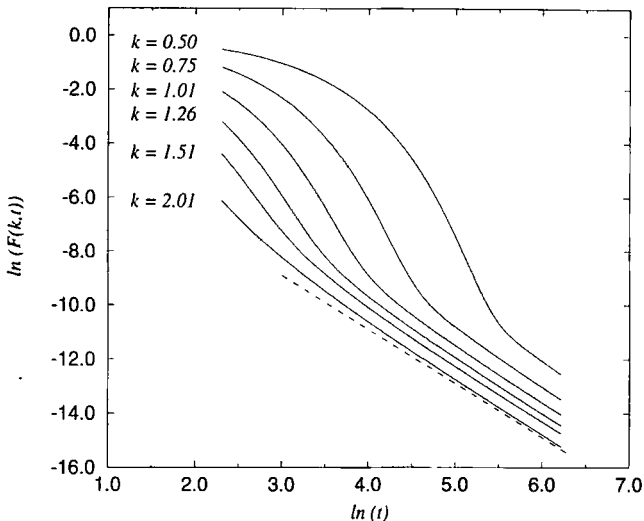


Fig. 7. Log-log plot of the self-dynamic structure factor $F(k, t)$ at various (large) k values in the two-dimensional system with broken-bond scatterers. The dashed line is a line with a gradient of -2 , provided for comparison.

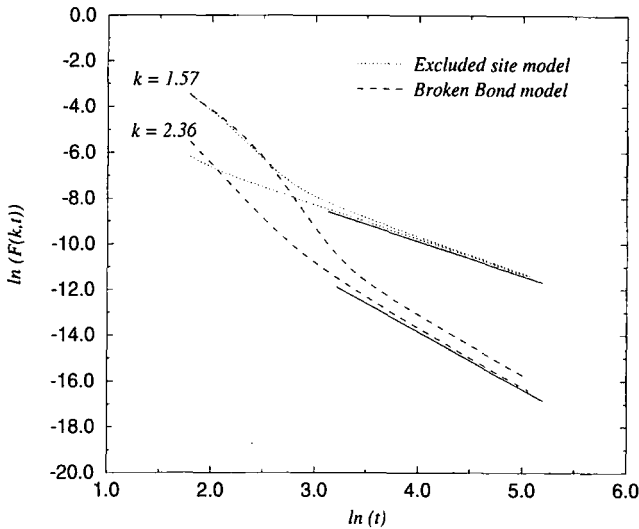


Fig. 8. Log-log plot of the self-dynamic structure factor $F(k, t)$ at two (large) k values for the three-dimensional excluded-site model (dotted lines) and broken-bond model (dashed lines). The upper solid line is a line with a gradient of -1.5 and the lower solid line a line with a gradient of -2.5 . These are provided for comparison.

bonds, again well below the critical density. The results are plotted in log-log form in Fig. 8. Again we see an asymptotic power-law decay; this time the exponents are -1.5 (for the excluded-site model) and -2.5 (for the broken-bond model). In each case the decay is half a power faster than the equivalent decay in two dimensions. The coefficient of the tail for the excluded-site model appears to be independent of k , while for the broken-bond model the coefficient of the tail increases with decreasing k . This is the same kind of behavior that we observed in two dimensions.

4. DISCUSSION

By using the moment propagation technique it proved possible, with modest computational effort, to calculate the self-dynamic structure factor accurately enough to allow us to extract the time-dependent Burnett coefficient $B(t)$. By examining the time dependence of $B(t)$ it was possible to confirm theoretical predictions that the Burnett coefficient diverges logarithmically in two dimensions. The long-time tails we found in $F(k, t)$ were completely unexpected and have not, to our knowledge, been

predicted theoretically.³ Where these tails, if genuine, make a significant contribution to $F(k, t)$ it is clear that the cumulant expansion does not exist. Our results would imply that, at long times, the SDSF takes the form

$$F(k, t) \sim \frac{\beta_1}{t} \quad (20)$$

$$F(k, t) \sim \frac{\beta_2}{(kt)^2} \quad (21)$$

for the excluded-site and broken-bond models, respectively. In both cases β is a constant, independent of k . The interesting question is, how does the relative importance of this effect scale with time? If we introduce a dimensionless time parameter $\tau (=k^2Dt)$, then, on dimensional grounds, one would expect that Eq. (20) and (21) can be written as

$$F(k, \tau) \sim k^2 \frac{\gamma_1}{\tau} \quad (22)$$

$$F(k, \tau) \sim k^2 \frac{\gamma_2}{\tau^2} \quad (23)$$

respectively, with γ a constant independent of k . In terms of τ the short-time exponential decay of $F(k, t)$ is independent of k . This suggests that, in both cases, the tail becomes less important at smaller values of k .

To summarize, the divergence of the Burnett coefficient tells us that, in two-dimensional Lorentz gases, Fickian behavior is never reached. Our results would also suggest that not only is the distribution not Gaussian at long times, but neither can it be expanded about a Gaussian, other than in the limit of small k .

ACKNOWLEDGMENTS

We thank Matthieu Ernst for pointing out to us the relevant theoretical predictions. Along with our thanks, we would also like to send both our

³ Since submitting this article it has been pointed out to us by J. Machta that the mode-coupling theory proposed by Ernst *et al.*¹²⁴⁾ does in fact predict a power-law decay of the self-dynamic structure factor. This was not, it appears, appreciated at the time. Furthermore, the theory predicts power-law exponents in precise agreement with the simulations for both the excluded-site and broken-bond models. A recent calculation by H. van Beijeren suggests that the tails can also be explained in a simple way by considering random walks excluded by the presence of a single scatterer. A detailed comparison between theoretical values for the amplitude of the tails and simulation results is currently underway. Preliminary results indicate excellent agreement.

best wishes and congratulations. Many thanks are also due to Andrew Masters for his helpful observations, and to J. Machta and H. van Beijeren for bringing to our attention recent theoretical developments. The (speedy) comments on the manuscript of Maarten Hagen and Paolo Teixeira were also much appreciated. The work of the FOM Institute is part of the scientific program of FOM and is supported by the Nederlandse Organisatie voor Wetenschappelijk Onderzoek (NWO). Computer time on the CRAY-C98/4256 at SARA was made available by the Stichting Nationale Computer Faciliteiten (Foundation for National Computing Facilities).

REFERENCES

1. B. J. Alder and T. E. Wainwright, *Phys. Rev. A* **1**:18 (1970).
2. M. H. Ernst, E. H. Hauge, and J. M. J. van Leeuwen, *Phys. Rev. Lett.* **25**:1254 (1970).
3. M. A. van der Hoef and D. Frenkel, *Phys. Rev. A* **41**:4277 (1990).
4. M. A. van der Hoef and D. Frenkel, *Physica D* **47**:191 (1991).
5. M. A. van der Hoef and D. Frenkel, *Phys. Rev. Lett.* **66**:1591 (1991).
6. P. M. Binder and D. Frenkel, *Phys. Rev. A* **42**:2463 (1990).
7. C. P. Lowe and A. J. Masters, *Physica A* **195**:149 (1992).
8. C. P. Lowe and A. J. Masters, *Physica A* **214**:413 (1995).
9. M. Hagen, C. P. Lowe, and D. Frenkel, *Phys. Rev. E* **51**:4287 (1995).
10. C. P. Lowe, D. Frenkel, and A. J. Masters, *J. Chem. Phys.* **103**:1582 (1995).
11. C. P. Lowe and D. Frenkel, *Physica A* **220**:251 (1995).
12. J. R. Dorfman and E. G. D. Cohen, *Phys. Rev. Lett.* **25**:1257 (1970).
13. N. K. Ailawadi and B. J. Berne, *J. Chem. Phys.* **54**:3569 (1971).
14. A. J. C. Ladd, *J. Fluid. Mech.* **241**:311 (1994).
15. Y. W. Kim and J. E. Matta, *Phys. Rev. Lett.* **31**:208 (1973).
16. P. D. Fedele and Y. W. Kim, *Phys. Rev. Lett.* **44**:691 (1980).
17. G. L. Paul and P. N. Pusey, *J. Phys. A* **14**:3301 (1981).
18. C. Morkel, C. Gronemeyer, W. Gläser, and J. Bosse, *Phys. Rev. Lett.* **58**:1873 (1987).
19. J. X. Zhu, D. J. Durian, J. Müller, D. A. Weitz, and D. J. Pine, *Phys. Rev. Lett.* **68**:2559 (1992).
20. D. Frenkel and M. H. Ernst, *Phys. Rev. Lett.* **63**:2165 (1989).
21. M. J. Ernst and A. Weijland, *Phys. Lett. A* **34**:39 (1971).
22. B. J. Alder and W. E. Alley, *J. Stat. Phys.* **19**:341 (1978).
23. B. J. Alder and W. E. Alley, *Physica A* **121**:523 (1983).
24. M. H. Ernst, J. Machta, J. R. Dorfman, and H. van Beijeren, *J. Stat. Phys.* **34**:413 (1984).
25. P.-M. Binder, *Phys. Rev. E* **49**:R3565 (1994).
26. W. E. Alley, Ph.D. Thesis, University of California, Davis (1979).
27. E. G. D. Cohen and F. Wang, *Physica A* **219**:39 (1995).